

Force-constant changes and localized modes for iron impurities in cubic metals from Mössbauer-fraction measurements*

Donald G. Howard and Rudi H. Nussbaum

Portland State University, Portland, Oregon 97207

(Received 2 July 1973)

Precision Mössbauer-fraction measurements have been used in combination with Mannheim's impurity-lattice theory to determine impurity-host force-constant changes and anharmonicity parameters for Fe⁵⁷ in Cu, Pd, Pt, Au, Al, Nb, and Cr. Combining these with available data on host-phonon frequency distributions, the impurity dynamic-response functions have been calculated. The theory predicts the existence of localized modes in Cu, Pt, and Au. The possible existence of localized modes in V, Zn, and Ni is also discussed.

I. INTRODUCTION

In a previous paper¹ we reported on impurity-host force-constant changes and impurity anharmonicity parameters as obtained from an analysis of the temperature dependence of the Mössbauer fraction $f(T) = e^{-k^2 \langle x^2 \rangle_T}$ of Fe⁵⁷ in various cubic metal hosts. (k is the wave number of the resonant γ ray and $\langle x^2 \rangle_T$ the mean-squared displacement of the radiating atoms at temperature T .) At liquid-helium temperature our data were analyzed with the help of the zero-temperature limit of a simple-cubic-crystal model, with harmonic nearest-neighbor forces only, shear and compressional forces assumed to be equal.² At high temperatures the data could be compared (after correction for anharmonicity) with the classical limit of a face-centered-cubic nearest-neighbor calculation.³ In the latter model, however, allowable force-constant changes are limited to less than 15%, a condition not met in the systems studied.

Impurity-host force-constant changes derived from such restricted models using Debye temperatures for the host (obtained from specific-heat measurements or elastic constants) can be considered first estimates only.^{1,4-6} A physically more reliable interpretation of high-precision Mössbauer $f(T)$ data over a wide temperature range requires a more extended theory, valid at *all* temperatures and suitable for numerical analysis.

II. DEFECT-LATTICE DYNAMICS

An impurity theory for face-centered cubic (fcc) and body-centered cubic (bcc) hosts including force-constant changes was published at about the time that Ref. 1 was submitted. Mannheim and co-workers' theory⁷ makes use of the symmetry properties of fcc and bcc lattices, and it assumes harmonic central forces, limited to nearest-neighbor interactions both for the impurities and the host. It is, however, valid at all temperatures and with no limitation to the magnitude of impurity-host force-constant changes. This theory contains only one free parameter, the ratio of the effective near-

est-neighbor-impurity-host force constant to the host-host force constant λ'/λ . This parameter, together with the known impurity-host mass ratio M'/M determines the coupling of the impurity to the lattice vibrations of the host. The response of the impurity to the phonon spectrum of the host $G(\omega)$ appears in the theory as the modified spectrum (the *dynamic-response function*⁸) $G'(\omega)$:

$$G'(\omega) = (M/M')G(\omega)\{[1 + \rho(\omega)S(\omega)]^2 + [\frac{1}{2}\pi\omega G(\omega)\rho(\omega)]^2\}^{-1} + \delta(\omega - \omega_L)(M/M') \times \{\rho^2(\omega)T(\omega) + (M/M') - [1 + \rho(\omega)]^2\}^{-1}, \quad (1)$$

where

$$\rho(\omega) = (M/M') - 1 + (2\omega^2/\omega_{\max}^2)[1 - \lambda/\lambda'], \quad (1a)$$

$$S(\omega) = \oint \omega'^2 (\omega'^2 - \omega^2)^{-1} G(\omega') d\omega', \quad (1b)$$

$$T(\omega) = \omega^4 \int (\omega'^2 - \omega^2)^{-2} G(\omega') d\omega', \quad (1c)$$

and $\delta(\omega - \omega_L)$ is the Dirac δ function at the localized-mode frequency ω_L , provided a localized mode ($\omega_L > \omega_{\max}$) exists. The condition for a resonance or a localized mode is

$$1 + \rho(\omega)S(\omega) = 0. \quad (2)$$

The host-host force constant λ is related to the cut-off frequency ω_{\max} of the host through⁹ $\omega_{\max}^2 = 2\lambda/M$.

If $G(\omega)$ for the host is known (e.g., from dispersion relations obtained from inelastic-neutron-scattering experiments and optimized force-constant models¹⁰) the impurity mean-squared displacement $\langle x^2 \rangle_T$ can be obtained directly from the dynamic response function $G'(\omega)$:

$$\langle x^2 \rangle_T = \frac{\hbar}{2M'} \int_0^\infty \omega^{-1} \coth\left(\frac{\frac{1}{2}\hbar\omega}{k_B T}\right) G'(\omega) d\omega, \quad (3)$$

a relation identical to that for an atom in a pure host,^{8,11} provided $G'(\omega)$ is replaced by $G(\omega)$.

In a best-fit procedure of the theoretical $\langle x^2 \rangle_T$ values to the experimental data [from $-\ln f(T)$] the only adjustable parameter would be λ'/λ in Eq.

(1a), were it not for the necessary correction for anharmonicity. The anharmonic contribution to $\langle x^2 \rangle_T$ introduces a second free parameter $\epsilon(-2)$ into the fitting procedure^{1,12} (see Note added in proof).

Other observables like the mean-squared velocity $\langle v^2 \rangle_T$ which results in a temperature-dependent second-order Doppler shift in Mössbauer spectroscopy, can also be simply related to the dynamic response function⁷ $G'(\omega)$ (see Sec. VC).

III. REINTERPRETATION OF PUBLISHED DATA (Cu, Pd, Pt)

In the first three rows of Table I we list the recalculated impurity parameters M'/M , λ'/λ , $\epsilon(-2)$, and ω_L/ω_{\max} for the fcc metal hosts Cu, Pd, and Pt using Mannheim's theory,⁷ together with the temperature range of our $f(T)$ measurements, $f(295\text{ K})$, and the references used to obtain $G(\omega)$ for the host. The experimental techniques, the data, and the method used for data analysis have been described previously.^{1,12} The theoretical $\langle x^2 \rangle_T$ from Eq. (3), corrected for anharmonicity, gives an excellent fit within the uncertainties of the data points. In Fig. 1 we show a typical fit of Eq. (3) to the data points¹ for a Pt host. Another example can be found in Ref. 12 for Cr.

Several force-constant changes derived from the present analysis are considerably larger than the former estimates¹ based on rather limited impurity models.^{2,3} The anharmonicity parameters remained unchanged within their uncertainties (see Note added in proof).

The data for Ni can only be considered estimates due to the uncertainties in the absolute values and the limited temperature range of the available $f(T)$ data. (For further discussion see Sec. VA).

IV. NEW DATA (Au, Al, Nb, Cr)

A. Dual impurity sites in Au and Al

In the fcc hosts, Au and Al, the solubility of Co⁵⁷ is known to be very low. Even at the few ppm atomic concentration range used in our source studies,^{13,14} we found evidence for thermal instability of the substitutional solid solutions of isolated Co⁵⁷ impurities in Au and Al at intermediate temperatures. This is likely related to the fact that the size of the impurity atom Co is much smaller than the nearest-neighbor distance in the two hosts. These nearest-neighbor distances are almost identical in these hosts, while the mass ratios, on the other hand, represent two opposite extremes in Table I.

TABLE I. Fe⁵⁷ impurity force-constant changes and anharmonicity parameters.

Metal Host	f(T) measurements		Force constant changes λ'/λ			Anharmonicity parameter $\epsilon(-2)$ (10^{-4} K^{-1}) ^a	Localized mode ω_L/ω_{\max}	G(ω) Refs.
	T Range (K)	f(295 K)	$M'_{\text{Fe}}/M_{\text{host}}$	This work ^a	Others			
Cu	4-760	0.710 ± 0.003	0.89	1.39 ± 0.04	...	4.0 ± 0.5	1.05	b
Pd	20-730	0.660 ± 0.003	0.54	0.61 ± 0.01	0.42 ^c	1.3 ± 0.3	...	d
Pt	20-760	0.724 ± 0.004	0.29	0.77 ± 0.03	0.55 ^e	2.5 ± 0.2	1.17	f
Ni	630-670	0.80 ± 0.01	0.97	> 1.4	2-3 ^g	> 4	> 1.1 ^g	h
Au ⁴	290-600	0.583 ± 0.007	0.29	1.0 ± 0.1 ^a	...	(1.5)	1.37	j
Al ⁴	290-490	0.50 ± 0.05	2.12	0.63 ± 0.05	1.51, ^c 0.61 ^k	(0)	...	l
Cr	80-600	0.793 ± 0.005	1.10	0.80 ± 0.05	...	3.0 ± 0.5	...	m
Nb	290-800	0.659 ± 0.005	0.61	0.85 ± 0.02	...	1.5 ± 0.2	...	n

^aSee Note added in proof.

^bReference 10.

^cReference 23. The authors applied Mannheim's theory to their *absorber* data. For $G(\omega)$ they used Debye spectra, however. Their f value for Fe⁵⁷ in Al (0.71) probably does not represent the substitutional site (see Sec. IV A).

^dA four-nearest-neighbor model was fitted to the $\omega(\vec{k})$ data of A. P. Miiller and B. N. Brockhouse [Phys. Rev. Lett. **20**, 798 (1968)]. The resulting values for λ'/λ and $\epsilon(-2)$ are the same as those resulting from the eight-nearest-neighbor model *MP-2* of Miiller and Brockhouse [Can. J. Phys. **49**, 704 (1971)].

^eD. Raj and S. P. Puri, Phys. Lett. A **33**, 306 (1970). The authors used the data of Ref. 1 but neglected to correct for anharmonicity.

^fD. H. Dutton, B. N. Brockhouse, and A. P. Miiller, Can. J. Phys. **50**, 2915 (1972).

^gReference 19.

^hR. J. Birgeneau, J. Cordes, G. Dolling, and A. D. B. Woods, Phys. Rev. **136**, A1359 (1964).

ⁱSee Secs. IV A and IV B.

^jSee Appendix and Note added in proof.

^kReference 17. The authors measured the temperature dependence of the area of their spectrum. If we use $\theta(-2) = 390\text{ K}$ (Ref. 1) for Al instead of 428 K, their estimate of λ'/λ becomes 0.61, based on the simple model of Ref. 2.

^lG. Gilat and R. M. Nicklow, Phys. Rev. **143**, 487 (1966).

^mJ. L. Feldman, Phys. Rev. B **1**, 448 (1970); W. M. Shaw and L. D. Muhlestein, Phys. Rev. B **4**, 969 (1971).

ⁿY. Nakagawa and A. D. B. Woods, Phys. Rev. Lett. **11**, 271 (1963).

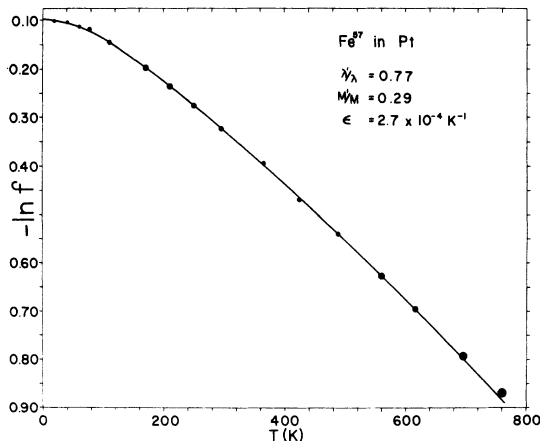


FIG. 1. Points are the experimental values of $-\ln f(T)$ for Fe^{57} in Pt. The solid line is $k^2 \langle x^2 \rangle_T [1 + \epsilon(-2)T]$ from Eq. (3) with the values of λ'/λ , M'/M , and $\epsilon(-2)$ as indicated in the insert.

At temperatures just below the melting points, the Co^{57} impurity atoms diffuse into *substitutional* sites,¹⁵ both in Au and in Al. These sites are characterized by near-natural width single-component line shapes in the Mössbauer spectrum.^{13,14} The single line reflects the local cubic symmetry of the substitutional sites, while the absence of broadening attests to the uniformity of the local environment of these sites. During long annealing times at temperatures below 1200 K (Au) or 820 K (Al), a fraction of the Co^{57} atoms slowly diffuse to an alternative site with a *drastically* reduced $\langle x^2 \rangle$ (at room temperature $f(\text{Au}) = 0.73$, $f(\text{Al}) = 0.77$).^{13,14} At each anneal temperature we found a definite equilibrium concentration of the impurity atoms in the two competing sites. The migration between the two sites was found to be reversible. There appears to exist in addition to the substitutional site only one type of alternative site for Co in our samples, characterized by a specific and uniform local environment but with noncubic local symmetry. This second site shows up in the Mössbauer spectrum as a clearly resolved quadrupole doublet, each component having near-natural width. In addition, there is a change in the isomer shift indicating a change in the *s*-electron density at the nucleus.^{13,14} The local structure of these impurity sites in Au and Al is not yet fully understood. The characteristic transition times between the substitutional and the alternative sites at various temperatures are quite different in Au as compared to Al, suggesting possibly different mechanisms in the formation and/or different structures of the noncubic impurity sites in these two hosts.

The 60% reduction of $\langle x^2 \rangle$ for the impurity atoms in the noncubic site of our Au and Al sources (com-

pared to that in the cubic substitutional site), the noncubic symmetry and yet uniformity of the local environment of these sites, as well as the large misfit between the size of the impurities and the lattice constants of either host, make the formation of *crowded clusters* involving a small number of impurities in off-lattice sites (possibly associated with vacancies and a local lattice distortion) a plausible hypothesis.¹³

An alternative explanation has been suggested, based on absorber studies with higher concentration alloys of Fe^{57} in Au. The appearance of doublet Mössbauer lines in those systems has been interpreted as being due to hyperfine interactions between impurities, clustering in *neighboring substitutional sites*.¹⁶ No reliable *f* measurements were done, however, on the two competing sites in those studies. The origin of these doublet lines and that of ours¹³ may therefore well be different. It is difficult to envisage such a large change in $\langle x^2 \rangle$ as we found, if it were the result of an interaction between two impurity atoms located in adjacent lattice sites but a distance apart far *exceeding* the size of the impurity atoms. If such a change were the result of greatly increased impurity-impurity binding, the clusters would not be expected to break up thermally below the melting point of the host.

Doublet spectra with varying splittings and isomer shifts have also been found in a number of studies of Fe in Al as *absorbers*, all of which involved considerably higher Fe concentrations.¹⁷ The doublets have been ascribed to impurity cluster formation. A recent study of the association of Al interstitials (after neutron irradiation) with substitutional Co^{57} impurity sites in *sources* also shows the appearance of a quadrupole doublet and an increase in *s*-electron density.¹⁸ No *f* measurements have been reported, however.

B. Force-constant changes in the substitutional sites of Au and Al

In addition to studying the thermal equilibrium of the two competing impurity sites in Au and Al,^{13,14} we measured $f(T)$ of the (single-line) *substitutional site* over a limited range of temperatures. The times required for collecting data at each temperature were kept short in comparison with the equilibrium formation times for the second site at those temperatures. However, from the analysis of line shapes after annealing near the melting point, we can only set an upper limit of 5–10% on the possible contribution from impurities in the high-*f* noncubic site for each $f(T)$ data point. Our $f(T)$ data for Au and Al can therefore be considered to be *upper bounds* to $f(T)$ for the substitutional sites. This implies that the values of λ'/λ listed in rows 5 and 6 of Table I can be interpreted as *upper bounds*.

The values of the anharmonicity parameters

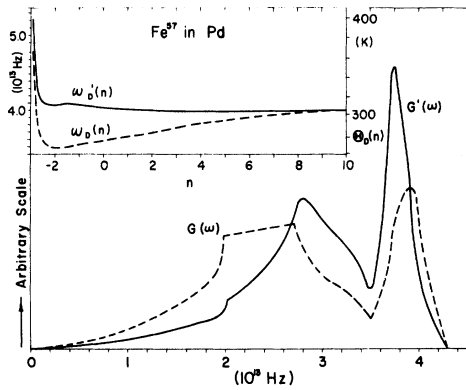


FIG. 2. Impurity response function $G'(\omega)$ and host phonon spectrum $G(\omega)$ for Fe^{57} in Pd. Insert: corresponding Debye moments.

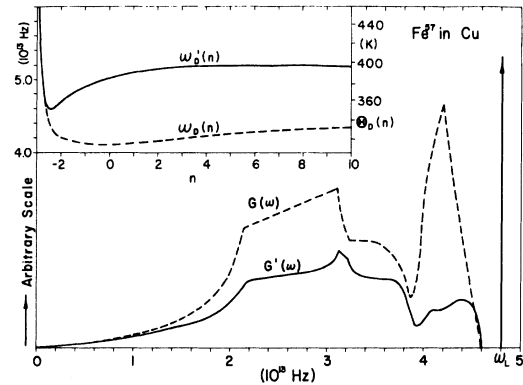


FIG. 5. Impurity response function $G'(\omega)$ and host phonon spectrum $G(\omega)$ for Fe^{57} in Cu. Insert: corresponding Debye moments.

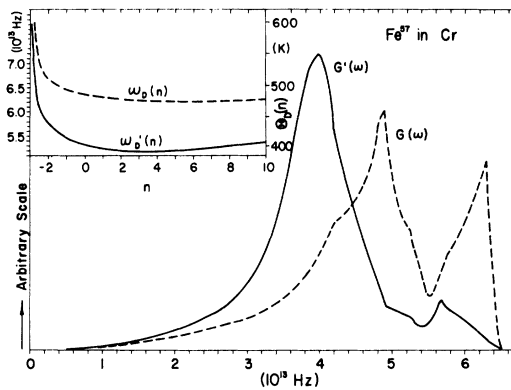


FIG. 3. Impurity response function $G'(\omega)$ and host phonon spectrum $G(\omega)$ for Fe^{57} in Cr. Insert: corresponding Debye moments.

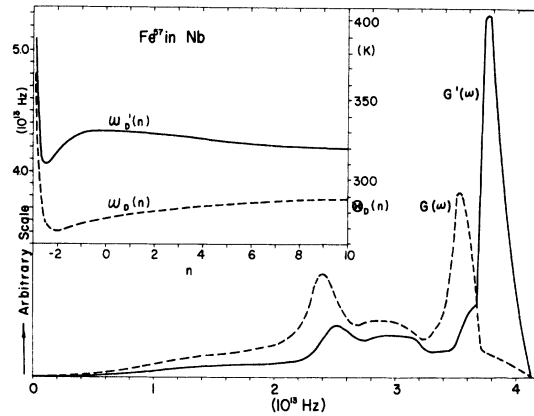


FIG. 6. Impurity response function $G'(\omega)$ and host phonon spectrum $G(\omega)$ for Fe^{57} in Nb. Insert: corresponding Debye moments.

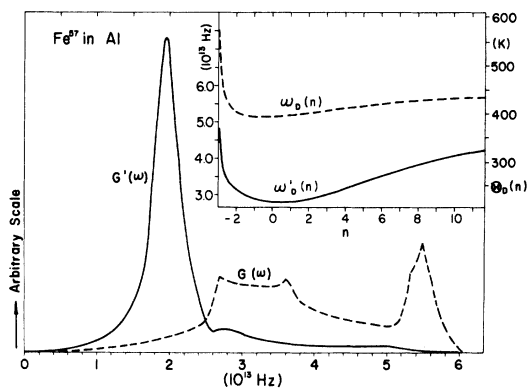


FIG. 4. Impurity response function $G'(\omega)$ and host phonon spectrum $G(\omega)$ for Fe^{57} in Al. Insert: corresponding Debye moments.

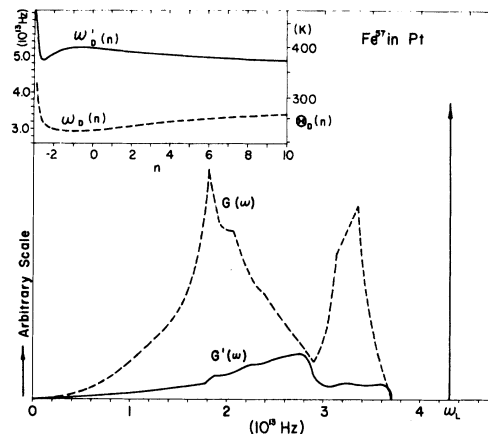


FIG. 7. Impurity response function $G'(\omega)$ and host phonon spectrum $G(\omega)$ for Fe^{57} in Pt. Insert: corresponding Debye moments.

$\epsilon(-2)$ for Au and Al could be affected considerably by a small admixture of high- f sites. This is indicated in Table I by parentheses.

Since the impurity theory used in this analysis is restricted to substitutional sites with cubic symmetry, only data derived from the $f(T)$ values for these sites have been included in Table I. [See Ref. c of Table I.]

C. Force-constant changes for Fe in Cr and Nb

In rows 7 and 8 of Table I the parameters for two bcc metals Nb and Cr have been added. The obtained fit of our $f(T)$ data for these hosts is equally good as that for the fcc hosts. The Cr data and their theoretical fitting have been published elsewhere¹² and are included in Table I for completeness. The $f(T)$ data on Nb were obtained from a source of Co⁵⁷ diffused into a single-crystal chip of Nb.

V. DISCUSSION

A. Impurity-host force-constant trends and comparisons with other data

1. *Trend in V.* A force constant ratio $\lambda'/\lambda \approx 2, 5$ has been reported⁷ for Fe in V. This is in remarkable contrast to the value of 0.80 found¹² for the neighboring host Cr (see Table I).

2. *Trend in Ni.* A recent analysis of $\langle v^2 \rangle_T$ measurements¹⁹ of Fe⁵⁷ in Ni (as absorber) yields $\lambda'/\lambda \approx 2-3$ predicting the existence of a localized mode. These data are consistent with our high-temperature $f(T)$ experiments.²⁰ If indeed the force-constant change is as large as Janot *et al.*¹⁹ estimate, our measurements would indicate an anomalously large anharmonicity parameter for this system.¹

3. *Trend in Zn.* A comparison of $f(T)$ data²¹ for Fe⁵⁷ in Zn with model calculations²² of $\langle x^2 \rangle_T$ in pure Zn, suggests that in this host also the force-constant ratio λ'/λ is considerably greater than unity. If Mannheim's theory could be extended to noncubic symmetry, a more detailed reevaluation could be done.

4. *Comparisons.* It is tempting to seek a correlation between the observed increases of impurity-host force constants in V, Ni, Cu, Zn, and Au and the decreases in Al, Cr, Nb, Pd, and Pt with the combined effects of relative atomic sizes,^{1,5} and the impurity and host electronic band structures. It seems plausible to assume that on the basis of size alone, the impurity-host force constant would be reduced where the impurity is small compared to the host nearest-neighbor distance. However, the electronic structure will enhance or reduce such trends. (Such an enhancement probably results in $\lambda'/\lambda \approx 1$ in Au.) The relevant parameters are yet unknown.

Various compilations of force-constant changes exist in the literature.^{1,4-6,23} In the sixth column of Table I we have included only those data which were obtained from $f(T)$ or $\langle v^2 \rangle_T$ studies over a range of temperatures using a theory applicable over this whole range. In comparing more recent impurity studies, the reliability of the host data used must also be considered, in particular, where tabulated Debye temperatures have been employed^{5,6,23} rather than experimentally derived phonon spectra. Few studies have applied the necessary corrections for anharmonic effects^{1,4,12} (see Note added in proof).

B. Impurity response functions $G'(\omega)$

1. In-band resonances in Al, Cr, Nb and Pd

Using Eq. (1) (Sec. II), we calculated $G'(\omega)$ for Fe⁵⁷ in Cu, Pd, Pt, Au, Al, Cr, and Nb. We used the available data for the host-phonon distribution functions, as referred to in the last column of Table I. (For Au see Appendix and Note added in proof.) These impurity response functions together with the host-phonon spectra $G(\omega)$ are plotted to the same scale in Figs. 2-8. Ni has not been included because of the rather large uncertainties in the impurity data (Secs. III and V A). In general, the low-frequency behavior of $G'(\omega)$ is determined by the mass ratio [as can be seen from Eq. (1a)]: for host atoms heavier than the Fe⁵⁷ impurity, such as Pd, Nb, Pt, and Au, $G'(\omega)$ is decreased, while for lighter host atoms, such as Al, $G'(\omega)$ is increased at low frequencies compared to the respective $G(\omega)$. Cu and Cr, where host and impurity mass are nearly the same, exhibit a $G'(\omega)$ at low frequencies almost identical to the host.

Large contributions to $G'(\omega)$ will occur at the roots of Eq. (2); these resonances may be either in-band or beyond the phonon cut-off frequency (localized mode). Both mass difference and force-constant difference can be expected to affect the position of these resonances. Mannheim [Ref. 7 (1972)] gives as a rule of thumb that the impurity resonance will appear near the band edge (ω_{\max}) if $\lambda'/\lambda \approx M'/\frac{1}{2}M$. For force-constant ratios smaller or larger than $M'/\frac{1}{2}M$ the resonance will appear inside the band, or as a localized mode, respectively. (Note that the relevant mass ratio for the position of the impurity resonance involves the *reduced* host mass.)

Using the above-mentioned criterion and the parameters of Table I from our analysis we would expect resonances in the vicinity of the band edge in Cu and Nb, while in Pd, Cr, and Al the peaks in $G'(\omega)$ should appear shifted toward lower and lower frequencies, respectively. In fact in Cu the resonance appears just above ω_{\max} (Fig. 5), while in Nb it falls just below it (Fig. 6). The qualitative features of the impurity response functions in Pd, Cr,

and Al, Figs. 2–4) agree well with those predicted by the above-mentioned rule of thumb.

2. Localized modes in Pt, Au, Ni, and Cu

Mannheim's criterion for the position of the impurity resonance (Sec. VB1) predicts well-localized modes in Pt and Au, with the latter at relatively higher frequency. Indeed, for Pt we find $\omega_L = 1.17 \omega_{\max}$ (Fig. 7), while for Au we find $\omega_L = 1.37 \omega_{\max}$ (Fig. 8). In addition, in Au more than 63% of the mean-squared displacement of the impurity atom is due to the localized mode at $T = 0$, decreasing to 37% at 600 K, a conclusion not substantially affected by the uncertainties in $f(T)$ referred to in Sec. IVB.

Mannheim's theory assumes harmonic forces only. Therefore, the localized modes appear in Figs. 5, 7, and 8 as Dirac δ functions. Anharmonic contributions to the interatomic forces, as well as other phonon interactions, are expected to broaden these sharp lines into narrow frequency bands. No data and only rough estimates²⁴ for these widths in metals are known to us. In view of this, the search for observable effects due to localized impurity modes remains of interest. Such effects on the Mössbauer spectrum depend critically on the thermal relaxation time of an excited localized mode in comparison with the nuclear lifetime.²⁵

3. Relation of $G'(\omega)$ to Debye theory

The deviation of a real phonon spectrum from a Debye spectrum is often displayed by means of a set of *Debye moments*^{1,10,11}

$$\omega_D(n) = \left(\frac{1}{5}(n+3) \int_0^\infty \omega^n G(\omega) d\omega \right)^{1/n} \text{ for } n > -3, n \neq 0. \quad (4)$$

We have calculated $\omega_D(n)$ for the host and $\omega'_D(n)$ for the Fe⁵⁷ impurity [replacing $G(\omega)$ with $G'(\omega)$ in Eq. (4)] for $-2.9 \leq n \leq 10$ and presented them in the *inserts* to Figs. 2–8. For comparison with other data we have also indicated the corresponding variation in *weighted Debye temperatures*^{1,11} $\Theta_D(n) = (\hbar/k_B)\omega_D(n)$. For a Debye spectrum $\omega_D(n) \equiv \omega_{\max}$. In the real crystals (Figs. 2–8), the (-3) moment is considerably larger than the (-2) moment. The (-3) moment depends on the coefficient of the initial quadratic part of the distribution.¹⁰ The dispersion inherent in a real lattice always causes the group velocity of phonons to be lower than the phase velocity in the vicinity of the Brillouin zone boundary, causing $G(\omega)$ to increase *above* that given by the initial quadratic term, and therefore an initial *decrease* in the moments above (-3) .

From $\omega'_D(n)$ in Figs. 2–4 it can be seen that Fe⁵⁷ in Pd comes closest to fitting a Debye model, while in Cr and Al the deviation becomes more pronounced. For Cu, Nb, Pt, and Au (Figs. 5–8), the $\omega'_D(n)$

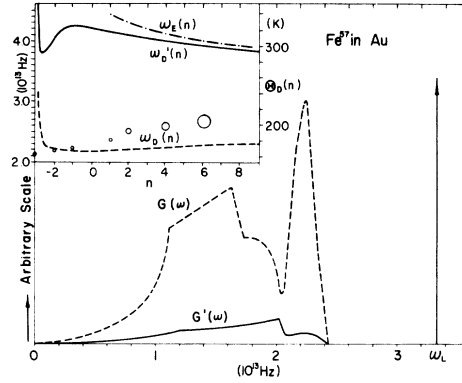


FIG. 8. Impurity response function $G'(\omega)$ and host phonon spectrum $G(\omega)$ for Fe⁵⁷ in Au (see Appendix). Insert: corresponding Debye moments $\omega'_D(n)$ and $\omega_D(n)$, and the calculated moments for a pure Einstein spectrum with frequency $\omega_E = \omega_L$ (see Sec. VB3). The circles are moments calculated from elastic data in Ref. 29.

curves show a growing addition of Einstein-like behavior [see the insert of Fig. 8 for a pure Einstein mode with $\omega_E = \omega_L$ so that $\omega_E(n) = (\frac{1}{5}n + 1)^{1/n} \omega_L$] reflecting the existence of a localized mode or a high frequency resonance. The effect of the localized mode in Pt is stronger than in Cu (see Figs. 5 and 7), consistent with our previous observation¹ that at low temperatures $\langle x^2 \rangle$ for Fe⁵⁷ in Pt seemed to fit a mixture between a Debye and an Einstein model.

C. Temperature dependence of isomer shifts

Mannheim's theory⁷ also allows the calculation of the mean-squared velocity $\langle v^2 \rangle_T$:

$$\langle v^2 \rangle_T = \frac{\hbar}{2M'} \int_0^\infty \omega \coth \left(\frac{1}{2} \frac{\hbar \omega}{k_B T} \right) G'(\omega) d\omega. \quad (5)$$

The quantity determines the second-order Doppler shift (SOD) $-\langle v^2 \rangle_T / 2c$ of the Mössbauer line. At high temperatures, $\langle v^2 \rangle_T$ becomes independent of the host (classical limit), and thus of force-constant changes. Sensitivity of $\langle v^2 \rangle_T$ to λ'/λ is greatest at $T = 0$. However, for Pd, e.g., a change in λ'/λ from 0.61 to 0.57, results in a change in SOD of only 0.002 mm/sec at $T = 0$ (about 1% of the natural linewidth), while the same change in the force constant results in a change in $f(600 \text{ K})$ of 3%, about three times the typical uncertainty in our measurements.¹ It appears to us, therefore, that the primary value of Eq. (5) lies in predicting the SOD with the help of the impurity parameters determined accurately from $f(T)$ measurements. Then, if high-precision temperature-shift measurements are available, the *temperature-dependent isomer shift* [equivalent to the temperature dependence of the s-electron density $\langle |\Psi_s(0)|^2 \rangle_T$] could be extracted by subtracting the SOD from the total shift,²⁶

provided dependable corrections for anharmonicity in $\langle v^2 \rangle_T$ could be applied at high temperatures (see Note added in proof).

VI. SUMMARY

Precision Mössbauer fraction measurements have been used to determine force constant changes at the Fe⁵⁷ impurity sites, as well as anharmonicity parameters. With the help of the impurity theory employed for this analysis and the best available data on the phonon spectra $G(\omega)$ of the host metals, we have calculated the impurity dynamic response functions $G'(\omega)$, showing impurity in-band resonances as well as localized modes. In some cases these localized modes contribute substantially to the vibrational motion of the impurity atoms.

ACKNOWLEDGMENTS

We thank Dr. M. Takeo for his continued interest and valuable assistance with theoretical interpretations, and C. F. Steen, A. Venkatachar, and B. F. Brace who have contributed significantly to the measurements as well as to the data analysis at various stages of the investigation.

APPENDIX: Fe⁵⁷ IN Au

Because of the large neutron-capture cross section of gold, neutron-scattering studies have not been done, and thus we do not have a host-phonon distribution for gold. However, neutron-scattering studies for silver suggest that the criterion of homologous forces holds very well between silver and copper.²⁷ The similarity in electronic structure between these two metals and gold suggest that perhaps the same criterion might be applied, and we could use the phonon distribution of copper for gold by applying a scaling factor

$$\omega_{Au}/\omega_{Cu} = (Ma^2)_{Cu}^{1/2}/(Ma^2)_{Au}^{1/2} = 0.504.$$

As a check on this value we have fitted the mean-squared displacement for Au¹⁹⁷ in gold.²⁸ The values obtained using the above ratio are slightly too large; a good fit can be obtained using a ratio of 0.53 instead and an anharmonicity parameter of $6 \times 10^{-4} \text{ K}^{-1}$.

The phonon distribution shown in Fig. 8 is therefore that of copper scaled by the factor 0.53. A comparison of the $\omega_D(n)$ graph in the insert to Fig.

8 with the values deduced from elastic-constant data by Skelton and Feldman²⁹ as indicated shows agreement for the (-1) and (-2) moments, which are the dominant ones for analysis of Mössbauer experiments.^{1,11} The agreement is poor for other moments, especially the (-3) moment.

Note added in proof. (a) The procedure for data analysis followed in Ref. 12 and in this paper utilizes $f(T)$ data over a wide range of temperatures. The method implies a number of approximations regarding anharmonic effects. (i) The density-of-states function $G(\omega)$ for the host is not affected by anharmonic contributions; i.e., $G(\omega)$ and ω_{max} are independent of temperature. Compared to the obtainable experimental precision of neutron dispersion experiments, this approximation is poor (see Ref. d, Table I). (ii) The deviation of the measured $\langle x^2 \rangle_T$ for the impurity from the predicted temperature dependence (according to harmonic theory⁷) is to be ascribed to *anharmonic contributions affecting solely the impurity atoms* as described by the parameter $\epsilon(-2)$ [see Eq. (3), Ref. 12]. (iii) As a consequence of the above it is assumed that the effective impurity-host force-constant ratio λ'/λ is independent of temperature. With these implied approximations our procedure leads to an *overestimate* of the effective force-constant ratios. If, alternatively, we eliminate the anharmonic correction, and thus the need for the parameter $\epsilon(-2)$, by limiting the analysis of $f(T)$ data at or near those temperatures for which $G(\omega)$ was determined for the host, we find for several of the metals of Table I a *reduction* in λ'/λ by about 10%. For Cu and Pt, however, the parameter λ'/λ evaluated above room temperature in this way may be lower by as much as 20–30%, with ω_L approximating ω_{max} . In general, the host anharmonicity appears in a change of $G(\omega)$ and ω_{max} , while the impurity-host anharmonicity may show up as a variation of λ'/λ with temperature. We will discuss this alternative method of data analysis and its consequences in greater detail in a subsequent paper. (b) Recent neutron scattering studies³⁰ show that the criterion of homologous forces does not hold for gold. In particular, the longitudinal modes are shifted toward higher frequency, causing ω_{max} to be about 20% higher than we have estimated. The resonance mode remains localized, but it is shifted toward lower frequency by about 5% and is thus only about $1.06\omega_{max}$. As a result, the force-constant ratio will be substantially less than that quoted in Table I, the corrected value being $\lambda'/\lambda \approx 0.62$.

*Work supported by National Science Foundation Research Grant No. GP-28880.

¹R. H. Nussbaum, D. G. Howard, W. L. Nees, and C. F. Steen, Phys. Rev. **173**, 653 (1968).

²W. M. Visscher, Phys. Rev. **129**, 28 (1963).

³A. A. Maradudin and P. A. Flinn, Phys. Rev. **126**, 2059 (1962).

⁴W. A. Steyert and R. D. Taylor, Phys. Rev. **134**,

- A716 (1964).
- ⁵S. M. Qaim, J. Phys. F 1, 320 (1971).
- ⁶G. P. Gupta and K. C. Lal, Phys. Status Solidi B 51, 233 (1971).
- ⁷P. D. Mannheim, Phys. Rev. 165, 1011 (1965); P. D. Mannheim and A. Simopolous, Phys. Rev. 165, 845 (1965); P. D. Mannheim and S. S. Cohen, Phys. Rev. B 4, 3748 (1971); P. D. Mannheim, Phys. Rev. B 5, 745 (1972).
- ⁸G. W. Lehman and R. E. DeWames, Phys. Rev. 131, 1008 (1963).
- ⁹In the nearest-neighbor approximation this relation is exact. If *all* neighbor interactions are included, a small correction factor $(1+Z)$ appears. Z contains the sum of the second and higher *even* neighbor to first-neighbor force-constant ratios [see Eq. (14) in Ref. 7 (1972)]. In our application of the theory we use frequency spectra for the hosts which have been derived from models containing higher than first-neighbor force constants (see, e.g., Ref. 10). We have, however, neglected the above-mentioned small correction to our Eq. (1a).
- ¹⁰E. C. Svensson, B. N. Brockhouse, and J. M. Rowe, Phys. Rev. 155, 619 (1967); R. M. Nicklow, G. Gilat, H. G. Smith, L. J. Raubenheimer, and M. K. Wilkinson, Phys. Rev. 164, 922 (1967).
- ¹¹L. S. Salter, Adv. Phys. 14, 1 (1965); R. H. Nussbaum, in *Mössbauer Effect Methodology*, edited by I. J. Gruverman (Plenum, New York, 1965), Vol. 2, p. 3.
- ¹²B. F. Brace, D. G. Howard, and R. H. Nussbaum, Phys. Lett. A 43, 336 (1973). The labels (a) and (b) in Fig. 1 should be reversed.
- ¹³Ch. F. Steen, D. G. Howard, and R. H. Nussbaum, Solid State Commun. 9, 865 (1971); appeared in corrected form in Solid State Commun. 10, erratum after p. 584 (1972).
- ¹⁴D. G. Howard, R. H. Nussbaum, C. F. Steen, and A. Venkatachar, Bull. Am. Phys. Soc. 16, 835 (1971); A. Venkatachar, M. S. thesis (Portland State University, 1971) (unpublished).
- ¹⁵R. D. Taylor found the magnetic moment for Fe⁵⁷ in the single-line site to be consistent with that expected for a substitutional site (private communication).
- ¹⁶B. Window, Phys. Rev. B 6, 2013 (1972); and private communication.
- ¹⁷K. Sørensen and G. Trumpy [Phys. Rev. B 7, 1791 (1973)] made a *source* study of the *single-line* site. They also list all references to *absorber* studies.
- ¹⁸W. Mansel, G. Vogl, and W. Koch, Phys. Rev. Lett. 31, 359 (1973).
- ¹⁹C. Janot and H. Scherrer, J. Phys. Chem. Solids 32, 191 (1971).
- ²⁰D. G. Howard and J. G. Dash, J. Appl. Phys. 38, 991 (1967).
- ²¹R. H. Housley and R. H. Nussbaum, Phys. Rev. 138, A753 (1965); W. Kündig, K. Ando, and H. Bömmel, Phys. Rev. 139, A889 (1965).
- ²²R. E. DeWames, T. Wolfram, and G. Lehman, Phys. Rev. 138, A717 (1965).
- ²³D. A. O'Connor, M. W. Reeks, and G. Skyrme, J. Phys. F 2, 1179 (1972).
- ²⁴W. M. Visscher, Phys. Rev. 134, A965 (1964).
- ²⁵J. G. Dash and R. H. Nussbaum, Phys. Rev. Lett. 16, 567 (1966); R. H. Nussbaum and J. G. Dash, Phys. Status Solidi 19, K31 (1967).
- ²⁶R. M. Housley and F. Hess, Phys. Rev. 164, 340 (1967).
- ²⁷W. A. Kamitakahara and B. N. Brockhouse, Phys. Lett. A 29, 639 (1969).
- ²⁸D. J. Erickson, L. D. Roberts, J. W. Burton, and J. O. Thompson, Phys. Rev. B 3, 2180 (1971).
- ²⁹E. F. Skelton and J. L. Feldman, Acta Cryst. A 27, 484 (1971).
- ³⁰J. W. Lynn, H. G. Smith, and R. M. Nicklow, Phys. Rev. B 8, 3493 (1973).